

Degradation-relaxation phenomenology in nanocomposites: On the linearized kinetics crossover

Valentina Balitska, Oleh Shpotyuk, and Michael Brunner

Citation: *AIP Conference Proceedings* **1981**, 020161 (2018); doi: 10.1063/1.5046023

View online: <https://doi.org/10.1063/1.5046023>

View Table of Contents: <http://aip.scitation.org/toc/apc/1981/1>

Published by the *American Institute of Physics*

Degradation-Relaxation Phenomenology in Nanocomposites: on the Linearized Kinetics Crossover

Valentina Balitska^a, Oleh Shpotyuk^{b,c*} and Michael Brunner^d

^aLviv State University of Life Safety, 35 Kleparivska str., Lviv, 79007, Ukraine

^bJan Dlugosz University in Czestochowa, 13/15, Armii Krajowej str., 42200, Czestochowa, Poland

^cVlokh Institute of Physical Optics, 23, Dragomanov str., 79005 Lviv, Ukraine

^dTechnische Hochschule Köln / University of Technology, Arts, Sciences 2, Betzdorfer Str., Köln, 50679, Germany

* Corresponding author: Tel. (032) 263-83-03; Fax: (032) 294-97-35; E-mail address: olehshpotyuk@yahoo.com

Abstract. Phenomenological models of degradation-relaxation kinetics are considered for jammed systems like structurally-inhomogeneous nanocomposites, exemplified, in part, by screen-printed Cu_{0.1}Ni_{0.1}Co_{1.6}Mn_{1.2}O₄ spinel ceramics with conductive Ag and Ag-Pd compound contacts. Nanoinhomogeneities due to Ag or Ag-Pd diffusants in a spinel environment are shown to define the governing kinetics of thermally-induced electrical degradation (at 170°C) obeying non-exponential behavior in negative relative resistance drift. Parameterization of this phenomenon (in part, determination of kinetics-responsible scaling exponent β) is shown can be simply performed within indirect linear least-square analysis applied to the generalized relaxation function presented in double-logarithmic plotting of variables. Crossover from stretched-exponential (stretching exponent $0 < \beta < 1$) to compressed-exponential (compressing exponent $\beta > 1$) degradation kinetics is revealed in these nanocomposites dependently on contacting diffusant materials, i.e. conductive Ag-Pd ($\beta = 0.58$) or Ag ($\beta = 1.68$) compounds.

Keywords: relaxation; stretched-exponential, compressed-exponential, kinetics, spinel.

PACS: 82

A great variety of metastable substances rapidly quenched from disordered far-from-equilibrium liquid state possesses internal stresses inevitably built in at a so-called jamming fluid-to-solid transition [1]. Examples of such jammed systems include structurally-inhomogeneous nanocomposites, such as foams and soft glasses, dense colloidal fractal gels, micellar polycrystals, concentrated emulsions, clay suspensions, polymer-matrix composites, nanoparticle-filled supercooled liquids and glassy polymer melts, polymer nanocomposites disturbed by internal stress, some kinds of metallic glasses (like Mg₆₅Cu₂₅Y₁₀, Zn₆₇Ni₃₃), etc. [1-9]. These out-of-equilibrium systems realize their functionality due to internal structural inhomogeneities frozen at atomic and/or sub-atomic length scales, which modify their physical-chemical properties and materials' response on different external activations. With tending towards equilibrium in the controlled parameter $N_\eta(t)$, such systems obey compressed-exponential relaxation (CER) kinetics (e.g. super-exponential), which is faster than simple exponential decay (SED):

$$N_\eta(t) \sim \exp \left[\left(-\frac{t}{\tau} \right)^\beta \right], \quad (1)$$

with compressing exponent $\beta > 1$ and characteristic degradation time τ varied (in dependence on scattering vector q as q^{-1} , instead of q^{-2} proper to conventional thermally activated diffusion [1]).

This unusual anomalous dynamics in structurally-inhomogeneous systems is explained in terms of ultraslow ballistic motion of intrinsic scatters (carriers of ballistic-like motion) under internal stress frozen at a so-called *jamming transition* [1]. The built-in stress fields are frozen around some structural inhomogeneities (such as agglomerates of embedded nanoparticles, atomic clusters, absorbed molecules, etc.) to counter reduction in an entropy due to interaction with surrounding. The compressing exponent β in (1) serves as a measure of these internal stresses developed in such jammed systems under their tending towards metastable state.

Conversely, the collapse of internal stresses in more equilibrium conditions approaching a supercooled liquid state causes substantial changes in the underlying degradation kinetics, which attains typical SED functional ($\beta = 1$):

$$N_{\eta}(t) \sim \exp\left(-\frac{t}{\tau}\right). \quad (2)$$

This *CER-to-SED crossover* is well realized in *soft jammed systems*, where carriers of diffusive-like motion prevails ($\beta=1$), such as supercooled liquid-like polymers filled with “hard” filler nanoparticles (diffusants) [3-6]. In its preferential occurrence, this CER-to-SED crossover seems to be thermally-activated, being realized near glass transition temperature T_g , showing hyper-diffusive behavior (viz. CER) at low temperatures ($T < T_g$) and SED dynamics at high ones ($T > T_g$).

More specifically, in many structurally-dispersive systems, wide variety of characteristic times τ changes the degradation kinetics to stretched-exponential relaxation (SER) with $0 < \beta < 1$ (sub-exponential relaxation), which is slower than SED kinetics determined by (2). As a results, the temperature variation over out-of-equilibrium (glassy-like) and close-to-equilibrium (supercooled-liquid) states is hallmarked in universal dynamical *thermally-activated CER-to-SER kinetics crossover*, as it occurs, e.g., in different types of metallic glasses [6,7]. Alternatively, the degradation kinetics walking over these metastable glassy-like and supercooled-liquid states can be traced via physical ageing (the process evolving the system evolution from as-prepared rejuvenated to more relaxed equilibrium state [7]), as it is character for colloidal suspensions of Laponite [8,9]. Thus, the spontaneously aged colloidal suspensions were always characterized by the SER kinetics with $\beta < 1$ (varying around 0.5-0.8 in dependence on waiting times t), while the CER behavior with compressing exponent $\beta > 1$ (varying around ~ 1.5 in dependence on waiting times t) was found for the same samples after rejuvenation procedure [8].

Thereby, at a global scale, we can balance over these *aging-* and *thermally-activated CER-to-SER crossovers*, describing both types of non-exponential kinetics using the above eq. (1) as a unified master equation with *scaling exponent* β (viz. *non-exponentiality index*) attaining all positive β values, i.e. $0 < \beta < 1$ for stretching (SER) and $\beta > 1$ for compressing (CER) dependences. From a simplification point, the numerical parameterization of this generalized approach describing degradation kinetics by eq. (1) can be linearized in double-logarithmic plotting of variables:

$$\ln\left[-\ln N_{\eta}(t)\right] \sim \beta \ln t - \beta \ln \tau. \quad (3)$$

In this work, we shall apply this linearization approach to analyze other representative of this CER-to-SER kinetics crossover [10,11], revealed in thermally-induced electrical degradation in screen-printed structures of spinel-type $(\text{Cu,Ni,Co,Mn})_3\text{O}_4$ manganites with different diffusants, these being c Ag- and/or Ag-Pd compounds (*diffusant-dependent CER-to-SER kinetics crossover*).

EXPERIMENTAL

The degradation effects were studied in spinel-type $\text{Cu}_{0.1}\text{Ni}_{0.1}\text{Co}_{1.6}\text{Mn}_{1.2}\text{O}_4$ thick films prepared by screen-printing as described in more details elsewhere [12]. The starting ceramics were sintered (1040°C) using carbonate hydroxides and hydrates of the corresponding transition metals [13]. The paste was prepared by mixing the powdered $\text{Cu}_{0.1}\text{Ni}_{0.1}\text{Co}_{1.6}\text{Mn}_{1.2}\text{O}_4$ ceramics with MB-60 glass, Bi_2O_3 binder and some organic vehicle. Then, the paste was printed on alumina substrates (Rubalit 708S) with conductive Ag- or Ag-Pd layer (preliminary printed from C1216 paste). In final, these structures were fired at 850°C. The prepared thick-film spinel-metallic composites were subjected to degradation testing at 170°C by subsequent cycling (24-360 hours). The confidence interval in the relative resistance drift (RRD), e.g. changes in electrical resistance $\Delta R/R_0$ of these structures measured under normal conditions, were no worse than $\pm 0.2\%$, and overall uncertainties in RRD measurements did not exceed $\pm 0.5\%$.

For adequate phenomenological description of the observed degradation-relaxation kinetics, the $\Delta R/R_0$ values were treated by *direct non-linear least-square fitting* to the generalized relaxation function presented as [11,14,15]:

$$N_{\eta}(t) = RRD = a \left(\exp\left[-\left(\frac{t}{\tau}\right)^{\beta}\right] - 1 \right), \quad (4)$$

where a stands for degradation amplitude, τ is time constant and β is *non-exponentiality index*.

The numerical values of a , τ and β parameters used in the above eq. (4) were calculated in such a way to minimize the mean-square deviations *err* of the experimental points from the model curve.

Apart from, these parameters were also extracted from *indirect linear least-square curve fitting* using linearized double-logarithmic functional (3). Under accepted uncertainties in the measured $\Delta R/R_0$ values, the final accuracy in the *non-exponentiality index* β was estimated to be ± 0.05 .

RESULTS AND DISCUSSION

The typical kinetics curves illustrating the normalized RRD values defined as $\Delta R/R_0 = N_\eta(t)$ in respect to eq. (4) in ceramics with screen-printed electrical contacts prepared of Ag or Ag-Pd compounds are depicted on Fig. 1.

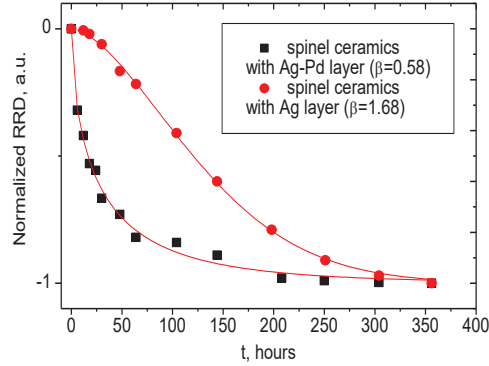


FIGURE 1. A comparative view of normalized kinetics corresponding to thermally-induced (170°C) degradation revealed by $\Delta R/R_0 = N_\eta(t)$ in $\text{Cu}_{0.1}\text{Ni}_{0.1}\text{Co}_{1.6}\text{Mn}_{1.2}\text{O}_4$ ceramics with screen-printed Ag-Pd (black squares) and Ag contact layers (red circles).

From visual inspection of this Fig. 1, it seems that tested degradation kinetics are essentially differ in their general occurrence for these cases. Indeed, the films with Ag-Pd contacts demonstrate sharp decreasing trend in the $N_\eta(t)$ with waiting time t ending by prolonged saturation at $t > 200$ h, thus obeying character SER functional shape with non-exponentiality index β approaching ~ 0.58 and effective time constant $\tau \cong 32$ h. Numerical values of both parameters were extracted from *direct non-linear least-square analysis* of the tested kinetics using eq. (4).

With changing in diffusant material on Ag (under transition to ceramics-Ag system), the initial decreasing trend in the control parameter $N_\eta(t)$ is depressed, being more stretched over shorter times $t < 30-40$ h. Then, this kinetics attained sharper decaying, resulting in saturation at longer waiting times $t > 250-300$ h. Thereby, the governing kinetics was drastically changed in this case, attaining an obvious *sigmoidal shape* character for CER curve [16] with fitting parameters β and τ (over-unity compressibility index $\beta = 1.68$ and time constant reaching $\tau \cong 154$ h).

In Fig. 2, the tested kinetics for screen-printed structures with Ag and Ag-Pd compound contacts are given in a general linearized presentation of double-logarithmic plotting (3). In this case, both β and τ parameters can be simply extracted from *indirect linear least-square analysis* as respective slope tangent and starting ordinate of the corresponding $y = \ln[-\ln N_\eta(t)] = f(\ln t)$ lines (shown in Fig. 2a and 2b). This procedure allows determination of $\beta = 0.58$ and $\tau = 32.5$ h for film with Ag-Pd contacts, and $\beta = 1.68$ and $\tau = 155.6$ h for that with Ag contacts.

The conductive material penetrating spinel ceramics is known to reduce its electrical resistivity resulting in negative RRD [12]. This diffusive process is thermally activated, in contrast to own changes, producing positive feedback in RRD due to increased defectiveness of ceramics [17]. The diffusive process quickly saturates with conductive material penetrating into ceramics as it character for $\text{Cu}_{0.1}\text{Ni}_{0.1}\text{Co}_{1.6}\text{Mn}_{1.2}\text{O}_4$ film with Ag-Pd contacts, which behaves as one “cumulative” diffusing agent with a significantly suppressed possibility for Ag atoms migration. The resulting kinetics of such diffusive degradation attains strong tendency to yield SER scenarios, as it is well illustrated by *non-linear least-square curve fitting* on Fig. 1 (black points) or *indirect linear least-square curve fitting* on Fig. 2a. However, if Ag penetration is not inhibited in ceramics by compounding with Pd (as for $\text{Cu}_{0.1}\text{Ni}_{0.1}\text{Co}_{1.6}\text{Mn}_{1.2}\text{O}_4$ films with contacts made of screen-printed Ag paste), the resulting kinetics is essentially changed. The Ag atoms can migrate in spaces between crystalline grains filled with glass binder, this first-stage diffusion process being quickly saturated via typical SER dependence (1) with $0 < \beta < 1$.

In terms of heterogeneity [18], the non-exponential kinetics can be described by heterogeneity factor h (the inverse $1/\beta$ value), giving degree of system deviation from simple SED kinetics (2). In our case, this parameter for SER kinetics is greater ($h = 1.72$), reflecting complex glassy process dominated by multiple local minima, while for CER kinetics, $h = 0.6$ due to non-exponential kinetics in Ag penetrating $\text{Cu}_{0.1}\text{Ni}_{0.1}\text{Co}_{1.6}\text{Mn}_{1.2}\text{O}_4$ ceramics. It should be admitted that Ag atoms penetrating spinel ceramics in a vicinity of intergranular boundaries create specific micron-sized bridges between grains, thus increasing electrical conductivity of a whole system.

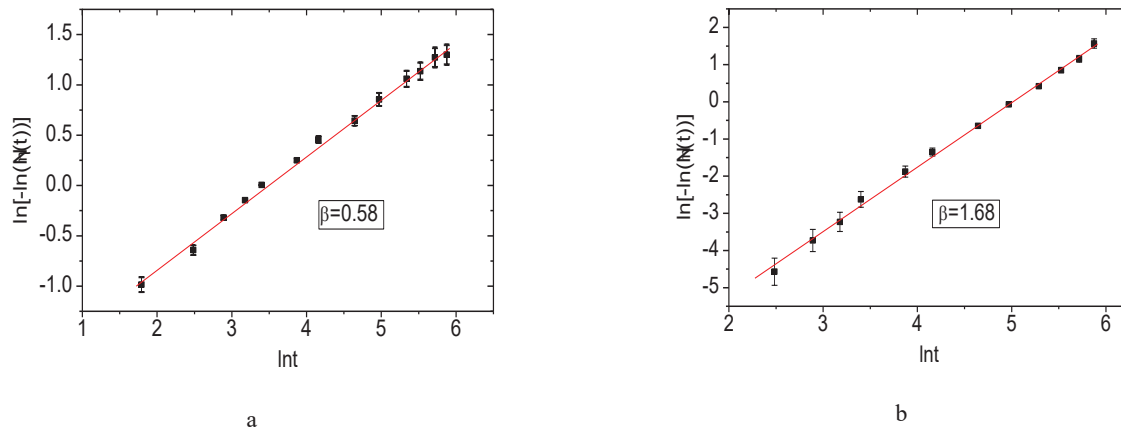


FIGURE 2. Generalized-linear presentation of kinetics corresponding to thermally-induced (170°C) degradation revealed by $\Delta R/R_0 = N_\eta(t)$ in spinel $\text{Cu}_{0.1}\text{Ni}_{0.1}\text{Co}_{1.6}\text{Mn}_{1.2}\text{O}_4$ thick-film ceramics with screen-printed Ag-Pd (a) and Ag contact layers (b).

In polymer nanocomposites such as polymethylmethacrylate capped Au [4] or Al_2O_3 particles [5] with scaling exponent β close to 1.4-1.9 (dependently on particle content), the CER kinetics appears at low temperatures below glass transition (*thermally-activated CER-to-SER crossover*). In rejuvenated colloidal glass [8-10], this crossover appears under physical ageing (*aging-induced CER-to-SER crossover*). The same order of β defined by *diffusant-dependent SER-to-CER kinetics crossover* for our thermally-relaxing systems, photo-switchable folded α -helix [19], rejuvenated colloidal glass [9-12] or polymer composites [5,6] testifies in favor of similarity in responsible models.

CONCLUSIONS

Principally different types of non-exponential degradation-relaxation kinetics are detected for the same spinel $\text{Cu}_{0.1}\text{Ni}_{0.1}\text{Co}_{1.6}\text{Mn}_{1.2}\text{O}_4$ thick-film ceramics in dependence on diffusants based on Ag or Ag-Pd compounds. If Ag migration is inhibited due to compounding with Pd as for conductive Ag-Pd alloy, the governing kinetics attains a stretched exponential behavior with scaling exponent β approaching ~ 0.58 . Under Ag penetration deeply into ceramics, as for spinel ceramics with Ag contacts, the resulting kinetics drastically changed attaining a compressed-exponential behavior with over-unity scaling exponent $\beta \sim 1.68$. This phenomenon of diffusant-dependent CER-to-SER kinetics crossover is simply parameterized within *indirect linear least-square analysis* applied to the generalized relaxation function presented in double-logarithmic plotting of variables.

REFERENCES

1. L. Cipelletti, L. Ramos, S. Manley, et al., M. Jahnsson, *Faraday Discuss* **123**, 237-251 (2003).
2. H. Guo, G. Bourret, M.K. Corbierre, et al., *Phys. Rev. Letter* **102**, 075702-1-075702-4 (2009).
3. C. Caronna, Y. Chushkin, A. Madsen, et al., *Phys Rev Letter* **100**, 055702-1-055702-4 (2008).
4. S. Srivastava, A.K. Kandar, J.K. Basu, et al., *Phys. Rev. E* **79**, 021408-1-021408-7 (2009).
5. R.A. Narayanan, P. Thiyagarajan, S. Lewis, et al., *Phys. Rev. Letter* **97**, 075505-1-075505-4 (2005).
6. B. Ruta, G. Baldi, G. Monaco, et al., *J. Chem. Phys.* **138**, 054508-1-054508-6 (2013).
7. B. Ruta, Y. Chushkin, G. Monaco, et al., *Phys. Rev. Lett.* **109**, 165701-1-165701-5 (2013).
8. R. Angelini, L. Zulian, A. Fluerasu, et al., *Soft Matter*. **9**, 10955-10959 (2013).
9. R. Angelini, E. Zaccarelli, F. Augusto, et al., *Nature Commun.* **5**, 4009-1-4009-7 (2014).
10. Y. Gueguen, V. Keryvin, T. Rouxel, et al., *Mechanics Mater.* **85**, 47-56 (2015).
11. V. Balitska, O. Shpotyuk, M. Brunner, et al., *Chem. Phys.* **501**, 121-127 (2018).
12. I. Hadzaman, H. Klym, O. Shpotyuk, *Int. J. Nanotechnol.* **11**, 843-853 (2014).
13. M. Vakiv, O. Shpotyuk, O. Mrooz, et al., *J. Europ. Ceram. Soc.* **21**, 1783-1785 (2001).
14. O. Shpotyuk, M. Brunner, I. Hadzaman, et al., *Nanoscale Res. Letters* **11**, 499-1-499-6 (2016)
15. O. Shpotyuk, V. Balitska, M. Brunner, *J. Phys. (Conf. Ser.)* **936**, 012050-1-012050-5. (2017)
16. D. Hamada, C.M. Dobson, *Protein Sci.* **11**, 2417-2426 (2002)
17. M. Vakiv, O.I. Shpotyuk, V.O. Balitska, et al., *J. Europ. Ceram. Soc.* **24**, 243-1246 (2004).
18. B. Gillespie, K.W. Plaxco, *Proc. Nat. Acad. Sci. USA* **97**, 12014-12019 (2000).
19. R. Hamm, J. Helbing, J. Bredenbeck, *Chem. Phys.* **323**, 54-65 (2006).